

Published in final edited form as:

*J Nucl Cardiol.* 2012 December ; 19(6): 1113–1123. doi:10.1007/s12350-012-9619-5.

## Prognostic value of quantitative high-speed myocardial perfusion imaging

Ryo Nakazato, MD, PhD<sup>\*</sup>, Daniel S. Berman, MD<sup>\*,†</sup>, Heidi Gransar, MSc<sup>\*</sup>, Mark Hyun, CNMT<sup>\*</sup>, Romalisa Miranda-Peats, MPH<sup>\*</sup>, Faith C. Kite, CNMT<sup>\*</sup>, Sean W. Hayes, MD<sup>\*,†</sup>, Louise E.J. Thomson, MBChB<sup>\*,†</sup>, John D. Friedman, MD<sup>\*,†</sup>, Alan Rozanski, MD<sup>‡</sup>, and Piotr J. Slomka, PhD<sup>\*,†</sup>

<sup>\*</sup>Departments of Imaging (Division of Nuclear Medicine) and Medicine (Division of Cardiology), Cedars-Sinai Heart Institute, Cedars-Sinai Medical Center, Los Angeles, CA, USA

<sup>†</sup>Departments of Medicine, David Geffen School of Medicine, University of California Los Angeles, Los Angeles, CA, USA

<sup>‡</sup>Division of Cardiology, St. Luke's Roosevelt Hospital, New York, New York, USA

### Abstract

**Background**—Most studies have reported using semi-quantitative analysis to assess the prognostic utility of SPECT myocardial perfusion imaging (MPI). Thus we studied the prognostic value of fully automated quantitative analysis software applied to new solid-state, high-speed (HS) SPECT-MPI.

**Methods**—1613 consecutive patients undergoing exercise or adenosine HS-MPI were followed for 2.6±0.5 years for all-cause mortality (ACM). Automated quantitative software was used for assessing stress total perfusion deficit (sTPD) and was compared to semi-quantitative visual analysis. MPI was characterized as 0% (normal); 1–4% (minimal perfusion defect); 5–10% (mildly abnormal); and >10% (moderately/severely abnormal).

**Results**—During follow-up, 79 patients died (4.9%). Annualized ACM increased with progressively increasing sTPD; 0% (0.87%), 1–4% (1.94%), 5–10% (3.10%) and >10% (5.33%) (log-rank  $p < 0.0001$ ). While similar overall findings were observed with visual analysis, only sTPD demonstrated increased risk in patients with minimal perfusion defects. In multivariable analysis, sTPD >10% was a mortality predictor (HR 3.03, 95% CI 1.30–7.09,  $p = 0.01$ ). Adjusted mortality rate was substantial in adenosine MPI, but low in exercise MPI (9.0% versus 1.0%,  $p < 0.0001$ ).

**Conclusions**—By quantitative analysis, ACM increases with increasing perfusion abnormality among patients undergoing stress HS-MPI. These findings confirm previous results obtained with visual analysis using conventional Anger camera imaging systems.

### INTRODUCTION

To date, most studies assessing the prognostic utility of single photon emission computed tomography (SPECT) myocardial perfusion imaging (MPI) have used semi-quantitative

---

Address for Correspondence: Piotr Slomka, PhD, Department of Imaging, Cedars-Sinai Medical Center, 8700 Beverly Boulevard, Taper Building Suite A047, Los Angeles, CA 90048, USA. Phone: 310-423-4348, Fax: 310-423-0171, slomkap@cshs.org.  
First author: Ryo Nakazato, MD, PhD, Cedars-Sinai Medical Center, 8700 Beverly Boulevard, Taper Building Room 1258, Phone: 310-423-4223, Fax: 310-423-0811, Ryo.Nakazato@cshs.org

Conflicts of interest: Dr. Piotr Slomka and Dr. Daniel Berman receive royalties from the software employed in the study. Dr. Daniel Berman is a shareholder in Spectrum-Dynamics. All others disclose no conflict of interest.

visual analysis, with relatively few studies reporting computer-based quantitative analysis (1–5). Furthermore, while new high-speed (HS) SPECT camera systems using cadmium-zinc-telluride (CZT) detectors have been introduced by various vendors (6–12) and have been validated by angiographic comparisons (13, 14), no prognostic study has been reported with this technology. Accordingly, in this study we evaluated fully automated myocardial perfusion analysis applied to HS-MPI and compared it to visual analysis for prediction of two to three year mortality rates.

## METHODS

### Study Patients

We evaluated 1766 consecutive patients who underwent HS-MPI at our center from September 2007 to October 2009, representing approximately 50% of the patients undergoing HS-MPI in our laboratory. Patients were referred for SPECT-MPI for clinical indications. From this initial population, we excluded 61 patients (3.4%) who were lost to follow-up due to missing or non-confirmed social security numbers, three patients with non-ischemic cardiomyopathy, three patients with post heart transplantation, and 34 patients who had dobutamine stress test. Fifty-two patients who underwent revascularization in the first 90 days after nuclear testing were also excluded (15), resulting in a final study population of 1613 patients. The research was approved by the Cedars-Sinai Medical Center institutional review board, and all subjects signed informed consent.

Prior to scanning, we collected information on the presence of categorical cardiac risk factors in each individual including hypertension, diabetes, hypercholesterolemia, smoking, and family history of early coronary heart disease as previously described (16). The occurrence of a prior myocardial infarction (MI) was based on patient history with confirmation by the patients' physician or documentation of acute MI from review of hospital electronic medical records. Cardiac symptoms were classified as previously described (15); asymptomatic, nonanginal pain, atypical angina, typical angina, and shortness of breath.

### Imaging and Stress Protocols

Patients were instructed to abstain from any products containing caffeine for 24 h before the test. Beta-blockers and calcium-channel antagonists were terminated 48 h before testing and nitrates were withheld for at least 6 h before testing. Stress testing was performed with a symptom-limited Bruce treadmill exercise protocol or vasodilator protocol (adenosine). For adenosine stress, adenosine was infused at 140  $\mu\text{g}/\text{kg}/\text{min}$  for 5 minutes and, when possible, low-level adjunctive treadmill exercise was performed during adenosine infusion. Twelve lead electrocardiogram (ECG) was monitored continuously during stress testing. An ischemic stress ECG response was defined as 1 mm horizontal or downsloping ST-segment depression or 1.5 mm upsloping ST depression. The full protocols have been previously described (13) and are summarized below.

**Rest/stress  $^{99\text{m}}\text{Tc}$ -sestamibi Protocol**—Rest/stress  $^{99\text{m}}\text{Tc}$ -sestamibi imaging (6) was performed in 1038 patients using weight-adjusted doses.  $^{99\text{m}}\text{Tc}$ -sestamibi [296–333 MBq (8–9 mCi)] was injected at rest. A 4-min rest image acquisition was performed in the upright position beginning 30 to 60 min after injection, followed by a 4-min supine acquisition in patients tested during the later period of the study. Patients then underwent symptom-limited standard exercise treadmill testing or adenosine stress with injection at peak stress of a weight-adjusted dose of  $^{99\text{m}}\text{Tc}$ -sestamibi [1332–1480 MBq (36–40 mCi)]. Beginning 15 to 30 min after stress injection, 2-min stress image acquisitions were performed in the upright and if supine stress imaging was performed, in the supine positions (6).

**Stress  $^{201}\text{Tl}$ /rest  $^{99\text{m}}\text{Tc}$ -sestamibi Protocol**—Stress  $^{201}\text{Tl}$ /rest  $^{99\text{m}}\text{Tc}$ -sestamibi imaging sequence (17) was used in 564 patients in whom patients were injected with  $^{201}\text{Tl}$  at peak stress. The specific weight-based dose regimen employed was to inject 74 MBq (2 mCi) in patients  $\leq 225$  lbs and 92.5 MBq (2.5 mCi) in patients  $>225$  lbs. Beginning approximately 10 min after exercise stress or 1 min after adenosine stress, a 6-min supine stress acquisition was performed followed by a 6-min upright acquisition. Subsequently, without moving the patient from the imaging chair,  $^{99\text{m}}\text{Tc}$ -sestamibi was injected [296 MBq (8 mCi) in patients  $\leq 225$  lbs and 370 MBq (10 mCi) in patients  $>225$  lbs], and beginning 2 min after injection, a 4-min rest upright acquisition was performed followed by a 4-min supine rest acquisition.

**Rest  $^{201}\text{Tl}$ /stress  $^{99\text{m}}\text{Tc}$ -sestamibi Protocol**—In 63 patients, a rest  $^{201}\text{Tl}$ /stress  $^{99\text{m}}\text{Tc}$ -sestamibi protocol was employed. A weight-based dose of  $^{201}\text{Tl}$  [74–148 MBq (2–4 mCi)] was injected at rest. A 6-min rest image acquisition was performed in the upright position within 15 min after  $^{201}\text{Tl}$  injection, followed by a 6-min supine acquisition in patients tested in the later period of the study. Patients then underwent symptom-limited standard exercise treadmill testing or adenosine stress with injection at peak stress of a weight-adjusted dose of  $^{99\text{m}}\text{Tc}$ -sestamibi [555–1295 MBq (15–35 mCi)]. Beginning 15 to 30 min after stress injection, 4-min stress image acquisitions were performed in the upright position in the supine position for those who also had supine stress imaging. The dual isotope protocol was used in early period of the study and is no longer employed in our laboratory.

### HS-SPECT Scanner and Imaging Method

A full description of the system performance of the HS-SPECT system used in this study (D-SPECT, Spectrum-Dynamics, Israel) has been previously reported (7, 18, 19). The system uses 9 tungsten collimated CZT detector columns rotating in synchrony, each consisting of 1024 ( $16 \times 64$ ), 5-mm thick CZT elements ( $2.46 \times 2.46$  mm). The size of the collimator holes matches the dimensions of the detector elements. Before imaging, the detector was positioned parallel to the patient's chest, with the heart in the center of the field of view. A 10-sec pre-scan acquisition was performed to identify the location of the heart and to set the angle limits of scanning for each detector column (region-of-interest centric scanning). Each image set was acquired with 120 projections per detector. Transaxial images were generated from list mode data by the use of a proprietary reconstruction algorithm based on the maximum likelihood expectation maximization method (19). No attenuation or scatter correction was applied. Images were then reoriented into short-axis and vertical and horizontal long-axis slices using standard software (QPS, Cedars-Sinai Medical Center, Los Angeles, California).

### Automated Quantification of HS-MPI

We use a separate normal database for each isotope as previously described (13). Briefly, normal limits for HS-SPECT were created from studies of 86 patients who had a low likelihood of CAD ( $<15\%$ ) based on age, sex, symptoms, coronary risk factor and results of treadmill stress test at the time of MPI (20): rest/stress  $^{99\text{m}}\text{Tc}$ -sestamibi ( $n = 60$ ) or stress  $^{201}\text{Tl}$ /rest  $^{99\text{m}}\text{Tc}$ -sestamibi ( $n = 26$ ). Patients did not have angina, shortness of breath, abnormal resting ECG, or abnormal stress ECG response. Additionally, as per previous practice in generating normal limits (21), the patients had normal rest and post stress HS-SPECT images by visual assessment of upright and supine images. In the rest/stress  $^{99\text{m}}\text{Tc}$ -sestamibi population, sex-specific normal limits were derived from a group of 60 patients (30 male, 30 female) with a low likelihood of CAD. In the stress  $^{201}\text{Tl}$ /rest  $^{99\text{m}}\text{Tc}$ -sestamibi population, sex-specific normal limits were derived from a group of 26 patients (15 male, 11 female) with a low likelihood of CAD. The automatically generated myocardial contours

were evaluated by an experienced imaging technologist without knowledge of any clinical data, and when necessary, contours were adjusted to correspond to the myocardium in 60 cases (3.7%). This was the only manual required step in this analysis. After this step, all 1613 studies were processed in a batch mode. The total automatic processing time for all cases was less than 1 hour (approximately 2 seconds per case). All results were automatically saved in Excel format to avoid any data entry errors. The quantitative perfusion variable employed was total perfusion deficit (TPD), which reflects a combination of both defect extent and severity of the defect in one parameter, as previously described (22), and provided by the QPS software. Stress perfusion defects on HS-MPI were assessed by quantification of the TPD (sTPD) (23, 24). Risk groups by sTPD were: sTPD 0% as normal; sTPD 1–4% as probably normal (minimal perfusion defect); sTPD 5–10% as mildly abnormal; and sTPD >10% as moderately/severely abnormal (based on previously established thresholds). Further, patients in the normal and probably normal sTPD group were sub-categorized as 0%, 1–<2% and 2–4%. Ischemic TPD (iTPD), which is the difference between sTPD and rest TPD, was also categorized in the same manner. Stress and rest left ventricular ejection fraction (LVEF) was quantified using a modified version of QGS (25) accounting for higher resolution and better visibility of the myocardial base (26). Stress LVEF >50% was considered as normal LVEF (27). We used only upright images for quantitative analysis in this study since not all patients had both upright and supine imaging (80%).

### Visual Scoring of HS-MPI

Visual segmental perfusion scores retrieved from the clinical reporting system were also used to estimate prognostic value by visual interpretation of HS-MPI. Visual scoring was performed by experienced imaging cardiologists during routine clinical reading using a 17-segment, five-point scoring system (0 = normal, 1 = equivocal, 2 = moderate, 3 = severe reduction of radioisotope uptake, and 4 = absence of detectable tracer uptake) (28) using all imaging data and patient history. Summed stress scores were obtained by adding the scores of the 17-segments of and was subsequently expressed as percentage of abnormal myocardium at stress (SSS%myo) by dividing the summed maximum score  $68 (4 \times 17)$  and multiplying by 100 as previously described (29). SSS%myo was expressed by categories: SSS%myo 0% = normal; SSS%myo 1–4% = probably normal (minimal perfusion defect); SSS%myo 5–10% = mildly abnormal; and SSS%myo >10% = moderately/severely abnormal (29). Similarly, percentage of ischemic myocardium (SDS%myo) was calculated by using summed difference score (SSS - summed rest score) and then categorized in the same manner.

### Follow-up

The endpoint of this study was all-cause mortality. Follow-up procedures were approved by the study center's institutional review board. Death status was ascertained by querying the Social Security Death Index in all patients. Survival was evaluated after a mean follow-up period of  $2.6 \pm 0.5$  years ( $31.8 \pm 6.6$  months, minimum 1 year).

### Statistical Analysis

All statistical calculations were performed using STATA (Version 11, StataCorp LP, College Station, Texas, USA) for Windows. Categorical variables are presented as frequencies and continuous variables as means  $\pm$  SD. Variables were compared with Pearson Chi-square test for categorical variables and by Student's two sample t-test for continuous variables. The annual event rate was calculated as the % number of events divided by person-years, was compared among groups using the log-rank test. Kaplan-Meier curves were generated in order to visually assess the survival in different groups. Cardiac symptoms were categorized as previously described (30); atypical angina, typical angina,

and shortness of breath were considered angina symptoms. Cox proportional hazards analysis was done to find predictors of all-cause death. Multivariable Cox regression analysis was performed that considered age, gender, hypertension, diabetes, prior CAD, angina symptoms and type of stress. The relationship between sTPD and SSS%myo were compared using Pearson's correlation and Bland-Altman analysis. A two-tailed  $p < 0.05$  was considered statistically significant. In each case, the proportional hazards assumption was assessed using Schoenfeld residuals.

## RESULTS

### Clinical Characteristics

The clinical characteristics of our patient population and a comparison of the patients who survived or died during follow-up period are shown in Table 1. At the completion of follow-up, 79 (4.9%) of our patients had died. Patients who died were older, had a higher frequency of prior CAD, MI, and hypertension, diabetes, and more often had adenosine stress. There was high correlation between sTPD and SSS%myo (Figure 1,  $r = 0.87$ ,  $p < 0.0001$ ). Comparison of the clinical characteristics of the patients undergoing adenosine vs. exercise stress is shown in Table 2.

### Mortality

Annualized mortality according to Kaplan–Meier survival curves by quantitative analysis is depicted in Figure 2. The Figure shows a progressive increase in mortality with worsening magnitude of sTPD. Overall, the annualized mortality rate was 0.87%, 1.94%, 3.10%, and 5.33% for sTPD of 0%, 1–4%, 5–10%, and >10%, respectively (log-rank test  $p < 0.0001$ ). There was significantly higher mortality in patients with sTPD 1–4% than in those with sTPD 0% (log-rank test  $p = 0.01$ ). In the subcategories of patients with normal and probably normal sTPD, the annualized mortality rate was 0.87%, 1.55% and 2.22% among the patients with sTPD of 0%, 1–<2% and 2–4%, respectively ( $p < 0.0001$ ). When the subcategory of sTPD 0% and 1–<2% were combined (sTPD <2%), the annualized mortality rate was 1.12%. With regard to iTPD, the annualized mortality was 1.29%, 2.03%, 4.76% and 3.43% among the patients with iTPD of 0%, 1–4%, 5–10% and >10%, respectively ( $p < 0.0001$ ).

Mortality according to Kaplan–Meier survival curves by visual analysis is depicted in Figure 3. There was a progressive increase in annualized mortality rate with worsening magnitude of SSS%myo. Overall, the annualized mortality rate was 1.26%, 2.06%, 4.15% and 5.62% for SSS%myo of 0%, 1–4%, 5–10% and >10%, respectively (log-rank test  $p < 0.0001$ ). There was no significant difference in mortality between patients with SSS%myo 0% and SSS%myo 1–4% (log-rank test  $p = 0.09$ ). The annualized mortality was 1.42%, 2.79%, 5.78% and 5.20% among the patients with SDS%myo of 0%, 1–4%, 5–10% and >10%, respectively ( $p < 0.0001$ ).

In 1613 patients, 1421 had normal stress LVEF ( $> 50\%$ ). In patients with normal stress LVEF, there was a progressive increase in annualized mortality rate with worsening magnitude of sTPD; 0.89%, 1.75%, 1.69% and 8.81% for sTPD of 0%, 1–4%, 5–10% and >10%, respectively (log-rank test  $p < 0.0001$ ). In patients with abnormal stress LVEF ( $n=192$ ), the annualized mortality rate was 0%, 3.67%, 8.26% and 3.11% for sTPD of 0%, 1–4%, 5–10% and >10%, respectively (log-rank test  $p = 0.1$ ). In those 192 patients, no patients died in sTPD of 0% and 7, 8 and 5 patients died in sTPD of 1–4%, 5–10% and >10%, respectively.

Case example is shown in Figure 4.



## Predictors of Mortality in Patients Undergoing HS-MPI

Table 3 shows the univariable predictors of mortality. Significant clinical variables included older age, hypertension, prior CAD and the use of adenosine stress. Significant MPI variables included the presence of minimal, mild and moderate/severe stress perfusion defect by quantitative analysis and the presence of mild and moderate/severe stress perfusion defect by visual analysis. In multivariable Cox regression analysis that adjusted for age, gender, hypertension, diabetes, prior CAD, angina symptoms and type of stress, the presence of moderate/severe abnormal quantitative stress perfusion defects was a significant predictor of all-cause mortality (Model 1, Table 4). Similarly in multivariable Cox regression analysis that adjusted for the same variables, the presence of mild and moderate/severe abnormal visual stress perfusion defects was a significant predictor of all-cause mortality (Model 2, Table 4).

## Comparison of Mortality among Patients Undergoing Exercise versus Adenosine MPI

There was a marked difference in mortality among patients undergoing exercise versus adenosine MPI. Death occurred in 9.0% of the patients undergoing adenosine MPI compared to only 1.0% of the patients undergoing exercise MPI ( $p < 0.001$ ). Patients undergoing adenosine stress were older than the patients who had exercise stress, had greater CAD risk burden, and a higher prevalence of prior CAD. After adjusting for age, gender, risk factors, prior CAD and angina symptoms, survival curve analysis for the patients undergoing exercise versus adenosine MPI indicated progressively worse survival among patients referred for adenosine stress compared to exercise stress ( $p < 0.0001$ , Figure 5).

## DISCUSSION

This is the first report evaluating the quantitative prognostic value of SPECT-MPI data obtained using a CZT detector camera. Using automated objective quantitative analysis, normal HS-MPI was associated objectively with a low annualized all-cause mortality rate and annualized mortality increased in proportion to stress MPI abnormality.

In our study the quantitative analysis of our MPI studies was fully automated. Of note, to date, there have been only sparse reports regarding the prognostic utility of SPECT-MPI according to quantitative analysis (1–5). In one case control prognostic analysis study of data from conventional cameras, visual and quantitative analysis have been shown to be equivalent (3). Accurate quantitative analysis, which is highly reproducible (31), affords an opportunity to eliminate observer variability and bias, provides an approach that is more generalizable to other centers than visual analysis, as it is not dependent on the expertise of the interpreter. This objective form of image analysis is particularly important for new devices which demonstrate slightly different image characteristics from those of conventional cameras.

Our findings using HS-MPI compare favorably with the results of stress MPI using the conventional Anger scintillation camera. When we divided our patients into those with normal (sTPD 0%), probably normal (sTPD 1–4%), mildly abnormal (sTPD 5–10%), and moderately/severely abnormal (sTPD >10%) stress perfusion defects, the annualized mortality rates were 0.87%, 1.94%, 3.10% and 5.33%, respectively. Previously, with conventional camera systems, we have reported a low annualized event rate (<1%/year) among patients with a normal stress MPI with an increase in event rate among patients manifesting a very mild perfusion defect (32).

In the current study, the quantitative analysis and visual analysis showed comparable overall findings with respect to predicting all-cause mortality. Interestingly, quantitative analysis

provided significant prognostic separation at the levels of risk at the low end of the spectrum (“normal” vs. “probably normal”) while visual analysis did not. We have reported a similar discrimination of increased risk of cardiac death using quantitative analysis when compared to visual analysis in patients with equivocal or minimally abnormal studies (3). These findings raise the possibility that there is a difference in the way expert observers interpret minor perfusion defects as equivocal compared to the way in which these defects are assessed by objective, quantitative software. The quantitative score of zero was associated with a lower event rate than the visual score of zero, but was seen in a much smaller proportion of the patients. When the subcategory of sTPD 1– <2% was considered abnormal, there was a trend toward increased mortality rates compared to the sTPD 0% group. When these two groups were combined, the annualized mortality rate was similar to that of a visual SSS%myo 0% (1.12% vs. 1.26%). A likely reason for the lower event rate in the quantitatively normal than in the visually normal scans is a tendency of imaging clinicians to score in the minimal decreases in uptake as zero, in order to reduce the use of equivocal categories of scan interpretation, with their associated uncertainty in clinical implication.

In patients with normal stress LVEF, the annualized mortality rate was progressively increased in annualized mortality with worsening magnitude of sTPD. In patients with abnormal stress LVEF, there was a trend toward increased mortality as a function of increasing sTPD; this trend did not reach statistical significance, most likely due to the small number of patients in this group.

A striking finding in our study was the marked difference in event rates in our exercise versus adenosine patients. Even though our sample size of exercise versus adenosine patients was comparable, only 1.0% of our exercise patients died compared to 9.0% of our adenosine patients during the same time period. Patients undergoing adenosine testing were older and had greater evidence of CAD or CAD risk burden, but adjusted survival curve analysis revealed a substantially higher mortality rate in the adenosine patients. Previously, it was demonstrated that adenosine patients have a substantially higher event rate than exercise MPI patients following matching of such patients based on age, gender, CAD risk factors and other clinical factors (33). Given this consistent difference, a case can be made for routinely separating outcome findings for exercise versus pharmacological MPI in future studies. This difference may be due to both poorer physical fitness and sedentary lifestyle and perhaps the presence of other mediating factors among patients undergoing pharmacological stress (33).

## Limitations

Our study contains a number of limitations. Since our study was performed at a single center, further study is needed to determine whether our findings will be applicable at other centers. However, our application of automated quantitative analysis in this study increases the likelihood that our results could be replicated elsewhere. We combined the use of different imaging protocols. The prognostic endpoint of the present study was all-cause mortality and did not include cardiac-specific death, myocardial infarction, unstable angina, or CAD-related hospitalization. While such assessment would be of importance, a proportional relationship between cardiac events and all-cause mortality has generally been observed among prognostic studies, and the assessment of all-cause mortality has the advantage of being free of ascertainment and verification bias (34). Information regarding co-morbidities, which may have confounded the findings, such as stroke, transient ischemic attack, peripheral vascular disease, chronic obstructive pulmonary disease, and malignancies were not available. The length of follow-up may have been too short to assess the impact of risk factors on clinical outcomes. Recent work by Supariwala et al. in this regard have demonstrated that CAD risk factors may be important in predicting long-term outcomes

following stress MPI (35). Importantly, we did not have data regarding medical treatment that followed from the performance of HS-MPI in our study. Thus, we could not evaluate whether aggressive medical therapy influenced the results of our study. The impact of medical therapies on downstream medical resource utilization and clinical outcomes has become increasingly assessed for newer technologies such as coronary artery calcium scanning (16) and coronary CT angiography (36, 37), but is presently understudied relative to stress MPI.

## CONCLUSION

In this first report of the prognostic value of HS-MPI by fully automated quantitative software, prognostic findings are comparable to those with visual analysis reported using conventional SPECT. Progressive abnormality on stress HS-MPI was associated with increasing all-cause mortality during two to three year follow-up.

## Acknowledgments

This research was supported in part by grant R01-HL089765 from the National Heart, Lung, and Blood Institute/National Institutes of Health (NHLBI/NIH) (PI: Piotr Slomka). Its contents are solely the responsibility of the authors and do not necessarily represent the official views of the NHLBI.

## References

1. Berman D, Kang X, Van Train K, Lewin H, Cohen I, Areeda J, et al. Comparative prognostic value of automatic quantitative analysis versus semiquantitative visual analysis of exercise myocardial perfusion single-photon emission computed tomography. *J Am Coll Cardiol*. 1998; 32:1987–95. [PubMed: 9857883]
2. Leslie WD, Tully SA, Yogendran MS, Ward LM, Nour KA, Metge CJ. Prognostic value of automated quantification of 99mTc-sestamibi myocardial perfusion imaging. *J Nucl Med*. 2005; 46:204–11. [PubMed: 15695777]
3. Xu Y, Nakazato R, Hayes S, Hachamovitch R, Cheng VY, Gransar H, et al. Prognostic value of automated vs visual analysis for adenosine stress myocardial perfusion SPECT in patients without prior coronary artery disease: a case-control study. *J Nucl Cardiol*. 2011; 18:1003–9. quiz 10-4. [PubMed: 21932154]
4. Dakik HA, Hwang WS, Jafar A, Kimball K, Verani MS, Mahmarian JJ. Prognostic value of quantitative stress myocardial perfusion imaging in unstable angina patients with negative cardiac enzymes and no new ischemic ECG changes. *J Nucl Cardiol*. 2005; 12:32–6. [PubMed: 15682363]
5. Shaw LJ, Cerqueira MD, Brooks MM, Althouse AD, Sansing VV, Beller GA, et al. Impact of left ventricular function and the extent of ischemia and scar by stress myocardial perfusion imaging on prognosis and therapeutic risk reduction in diabetic patients with coronary artery disease: Results from the Bypass Angioplasty Revascularization Investigation 2 Diabetes (BARI 2D) trial. *J Nucl Cardiol*. 2012; 19:658–69. [PubMed: 22527794]
6. Sharir T, Slomka P, Hayes S, DiCarli M, Ziffer J, Martin W, et al. Multicenter trial of high-speed versus conventional single-photon emission computed tomography imaging: quantitative results of myocardial perfusion and left ventricular function. *J Am Coll Cardiol*. 2010; 55:1965–74. [PubMed: 20430269]
7. Sharir T, Ben-Haim S, Merzon K, Prochorov V, Dickman D, Berman D. High-speed myocardial perfusion imaging initial clinical comparison with conventional dual detector angler camera imaging. *JACC Cardiovasc Imaging*. 2008; 1:156–63. [PubMed: 19356422]
8. Herzog BA, Buechel RR, Katz R, Brueckner M, Husmann L, Burger IA, et al. Nuclear myocardial perfusion imaging with a cadmium-zinc-telluride detector technique: optimized protocol for scan time reduction. *J Nucl Med*. 2010; 51:46–51. [PubMed: 20008999]
9. Buechel RR, Herzog BA, Husmann L, Burger IA, Pazhenkottil AP, Treyer V, et al. Ultrafast nuclear myocardial perfusion imaging on a new gamma camera with semiconductor detector technique: first clinical validation. *Eur J Nucl Med Mol Imaging*. 2010; 37:773–8. [PubMed: 20107783]



10. Esteves FP, Raggi P, Folks RD, Keidar Z, Askew JW, Rispler S, et al. Novel solid-state-detector dedicated cardiac camera for fast myocardial perfusion imaging: multicenter comparison with standard dual detector cameras. *J Nucl Cardiol*. 2009; 16:927–34. [PubMed: 19688410]
11. Slomka P, Patton J, Berman D, Germano G. Advances in technical aspects of myocardial perfusion SPECT imaging. *J Nucl Cardiol*. 2009; 16:255–76. [PubMed: 19242769]
12. Garcia EV, Faber TL, Esteves FP. Cardiac dedicated ultrafast SPECT cameras: new designs and clinical implications. *J Nucl Med*. 2011; 52:210–7. [PubMed: 21233190]
13. Nakazato R, Tamarappoo BK, Kang X, Wolak A, Kite F, Hayes SW, et al. Quantitative upright-supine high-speed SPECT myocardial perfusion imaging for detection of coronary artery disease: correlation with invasive coronary angiography. *J Nucl Med*. 2010; 51:1724–31. [PubMed: 20956478]
14. Duvall WL, Sweeny JM, Croft LB, Barghash MH, Kulkarni NK, Guma KA, et al. Comparison of high efficiency CZT SPECT MPI to coronary angiography. *J Nucl Cardiol*. 2011; 18:595–604. [PubMed: 21638154]
15. Hachamovitch R, Berman D, Shaw L, Kiat H, Cohen I, Cabico J, et al. Incremental prognostic value of myocardial perfusion single photon emission computed tomography for the prediction of cardiac death: differential stratification for risk of cardiac death and myocardial infarction. *Circulation*. 1998; 97:535–43. [PubMed: 9494023]
16. Rozanski A, Gransar H, Shaw LJ, Kim J, Miranda-Peats L, Wong ND, et al. Impact of coronary artery calcium scanning on coronary risk factors and downstream testing the EISNER (Early Identification of Subclinical Atherosclerosis by Noninvasive Imaging Research) prospective randomized trial. *J Am Coll Cardiol*. 2011; 57:1622–32. [PubMed: 21439754]
17. Berman D, Kang X, Tamarappoo B, Wolak A, Hayes S, Nakazato R, et al. Stress thallium-201/rest technetium-99m sequential dual isotope high-speed myocardial perfusion imaging. *JACC Cardiovasc Imaging*. 2009; 2:273–82. [PubMed: 19356571]
18. Patton J, Slomka P, Germano G, Berman D. Recent technologic advances in nuclear cardiology. *J Nucl Cardiol*. 2007; 14:501–13. [PubMed: 17679058]
19. Gambhir S, Berman D, Ziffer J, Nagler M, Sandler M, Patton J, et al. A novel high-sensitivity rapid-acquisition single-photon cardiac imaging camera. *J Nucl Med*. 2009; 50:635–43. [PubMed: 19339672]
20. Diamond G, Forrester J. Analysis of probability as an aid in the clinical diagnosis of coronary-artery disease. *N Engl J Med*. 1979; 300:1350–8. [PubMed: 440357]
21. Slomka PJ, Nishina H, Berman DS, Akincioglu C, Abidov A, Friedman JD, et al. Automated quantification of myocardial perfusion SPECT using simplified normal limits. *J Nucl Cardiol*. 2005; 12:66–77. [PubMed: 15682367]
22. Slomka P, Nishina H, Berman D, Akincioglu C, Abidov A, Friedman J, et al. Automated quantification of myocardial perfusion SPECT using simplified normal limits. *J Nucl Cardiol*. 2005; 12:66–77. [PubMed: 15682367]
23. Berman D, Kang X, Gransar H, Gerlach J, Friedman J, Hayes S, et al. Quantitative assessment of myocardial perfusion abnormality on SPECT myocardial perfusion imaging is more reproducible than expert visual analysis. *J Nucl Cardiol*. 2009; 16:45–53. [PubMed: 19152128]
24. Shaw L, Berman D, Maron D, Mancini G, Hayes S, Hartigan P, et al. Optimal medical therapy with or without percutaneous coronary intervention to reduce ischemic burden: results from the Clinical Outcomes Utilizing Revascularization and Aggressive Drug Evaluation (COURAGE) trial nuclear substudy. *Circulation*. 2008; 117:1283–91. [PubMed: 18268144]
25. Germano G, Kiat H, Kavanagh P, Moriel M, Mazzanti M, Su H, et al. Automatic quantification of ejection fraction from gated myocardial perfusion SPECT. *J Nucl Med*. 1995; 36:2138–47. [PubMed: 7472611]
26. Slomka P, Germano G, Kavanagh P, Javadi M, Berman D, Bengel F. Evaluation of a new automatic algorithm for quantification of ECG-gated 82Rb cardiac PET. *J Nucl Med*. 2009; 50 (Suppl 2):1167.
27. Sharir T, Germano G, Kang X, Lewin H, Miranda R, Cohen I, et al. Prediction of myocardial infarction versus cardiac death by gated myocardial perfusion SPECT: risk stratification by the

- amount of stress-induced ischemia and the poststress ejection fraction. *J Nucl Med*. 2001; 42:831–7. [PubMed: 11390544]
28. Berman D, Kiat H, Friedman J, Wang F, van Train K, Matzer L, et al. Separate acquisition rest thallium-201/stress technetium-99m sestamibi dual-isotope myocardial perfusion single-photon emission computed tomography: a clinical validation study. *J Am Coll Cardiol*. 1993; 22:1455–64. [PubMed: 8227805]
  29. Hachamovitch R, Hayes S, Friedman J, Cohen I, Berman D. Comparison of the short-term survival benefit associated with revascularization compared with medical therapy in patients with no prior coronary artery disease undergoing stress myocardial perfusion single photon emission computed tomography. *Circulation*. 2003; 107:2900–7. [PubMed: 12771008]
  30. Cheng VY, Berman DS, Rozanski A, Dunning AM, Achenbach S, Al-Mallah M, et al. Performance of the Traditional Age, Sex, and Angina Typicality-Based Approach for Estimating Pretest Probability of Angiographically Significant Coronary Artery Disease in Patients Undergoing Coronary Computed Tomographic Angiography: Results From the Multinational Coronary CT Angiography Evaluation for Clinical Outcomes: An International Multicenter Registry (CONFIRM). *Circulation*. 2011; 124:2423–32. [PubMed: 22025600]
  31. Xu Y, Hayes S, Ali I, Ruddy TD, Wells RG, Berman DS, et al. Automatic and visual reproducibility of perfusion and function measures for myocardial perfusion SPECT. *J Nucl Cardiol*. 2010; 17:1050–7. [PubMed: 20963537]
  32. Abidov A, Hachamovitch R, Hayes SW, Friedman JD, Cohen I, Kang X, et al. Are shades of gray prognostically useful in reporting myocardial perfusion single-photon emission computed tomography? *Circ Cardiovasc Imaging*. 2009; 2:290–8. [PubMed: 19808609]
  33. Rozanski A, Gransar H, Hayes SW, Friedman JD, Hachamovitch R, Berman DS. Comparison of long-term mortality risk following normal exercise vs adenosine myocardial perfusion SPECT. *J Nucl Cardiol*. 2010; 17:999–1008. [PubMed: 21076898]
  34. Lauer MS, Blackstone EH, Young JB, Topol EJ. Cause of death in clinical research: time for a reassessment? *J Am Coll Cardiol*. 1999; 34:618–20. [PubMed: 10483939]
  35. Supariwala A, Uretsky S, Singh P, Memon S, Khokhar SS, Wever-Pinzon O, et al. Synergistic effect of coronary artery disease risk factors on long-term survival in patients with normal exercise SPECT studies. *J Nucl Cardiol*. 2011; 18:207–14. [PubMed: 21184207]
  36. Min JK, Gilmore A, Budoff MJ, Berman DS, O'Day K. Cost-effectiveness of coronary CT angiography versus myocardial perfusion SPECT for evaluation of patients with chest pain and no known coronary artery disease. *Radiology*. 2010; 254:801–8. [PubMed: 20177094]
  37. Ladapo JA, Jaffer FA, Hoffmann U, Thomson CC, Bamberg F, Dec W, et al. Clinical outcomes and cost-effectiveness of coronary computed tomography angiography in the evaluation of patients with chest pain. *J Am Coll Cardiol*. 2009; 54:2409–22. [PubMed: 20082932]

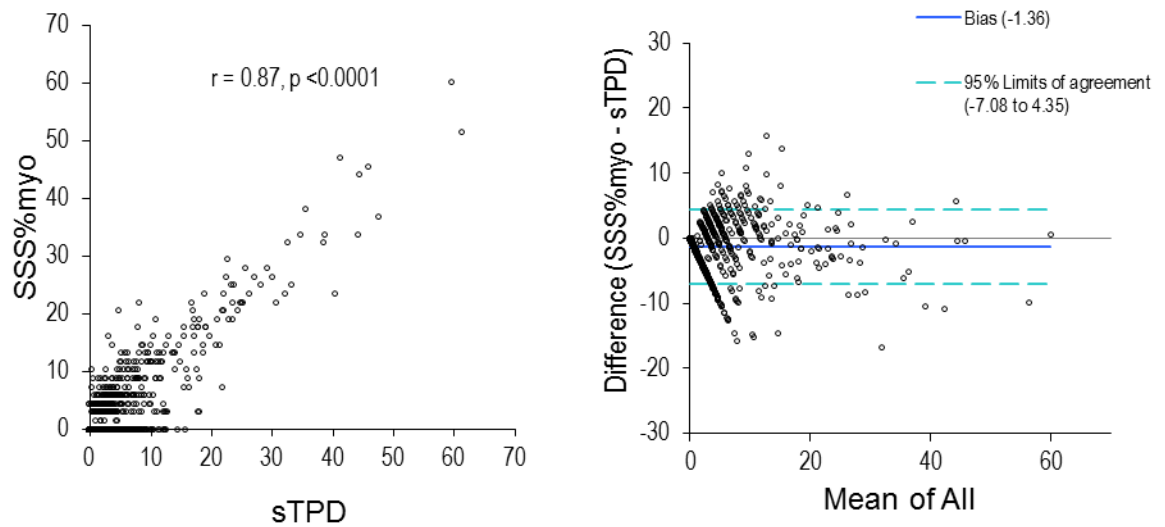


**Figure 1.** Correlation and Bland-Altman plot between sTPD and SSS%myo. *sTPD*, stress total perfusion deficit; *SSS%myo*, summed stress scores as a percentage of abnormal myocardium.

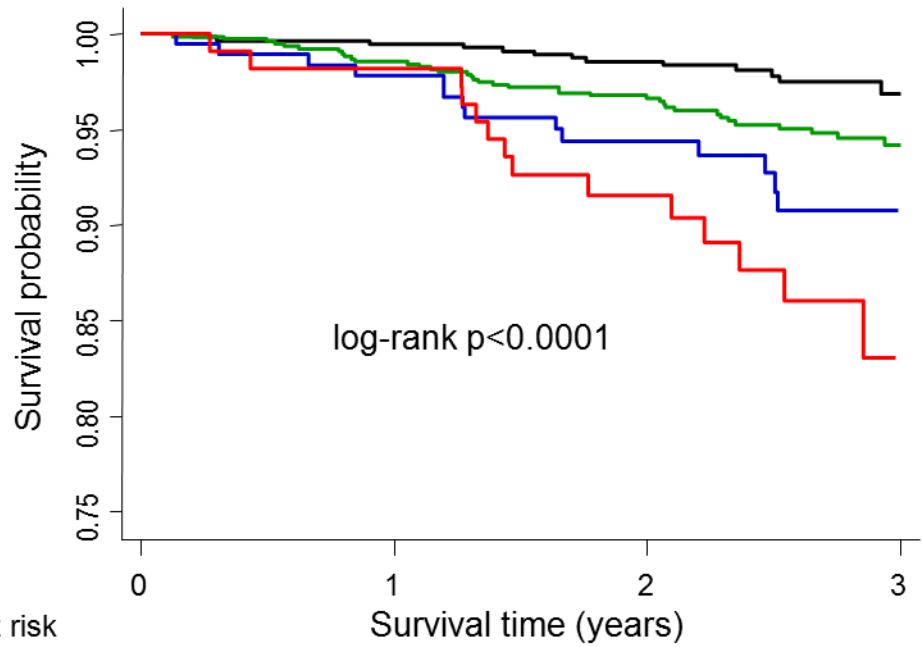
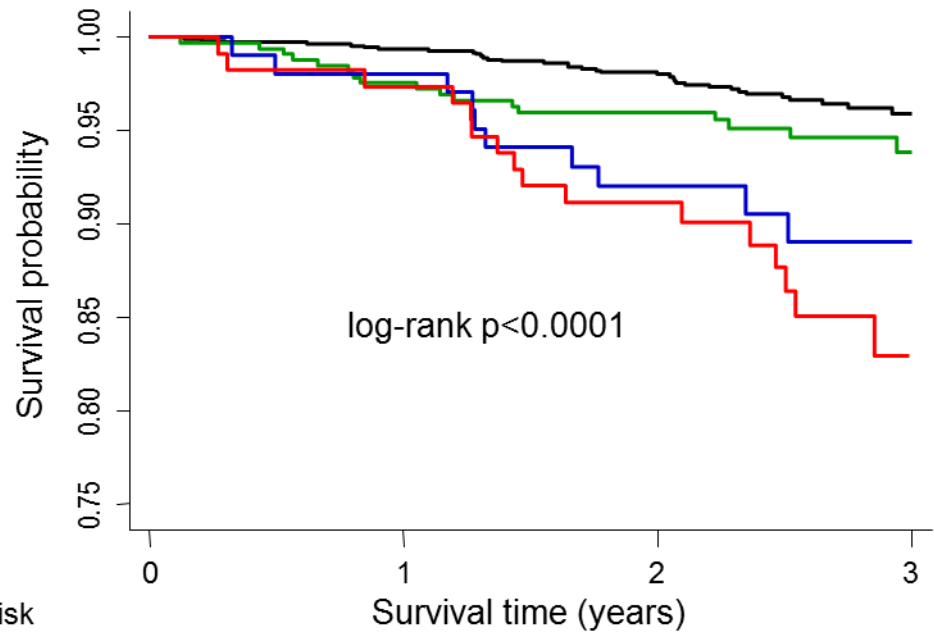


**Figure 2.** Kaplan–Meier survival curves for all-cause mortality in all patients by sTPD.



Number at risk	Survival time (years)			
	0	1	2	3
SSS%myo 0%	1075	1068	905	262
SSS%myo 1-4%	323	315	241	110
SSS%myo 5-10%	102	100	85	32
SSS%myo >10%	113	110	87	29

**Figure 3.** Kaplan–Meier survival curves for all-cause mortality in all patients by SSS%myo.



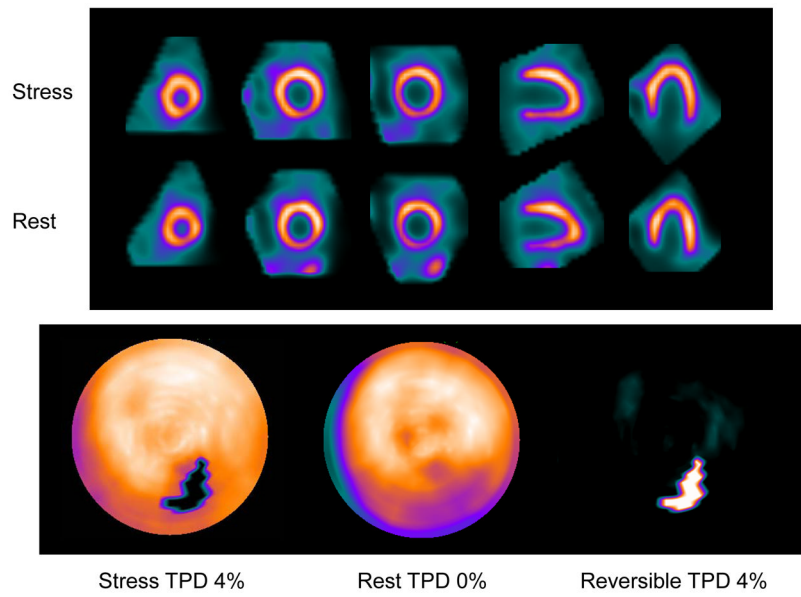
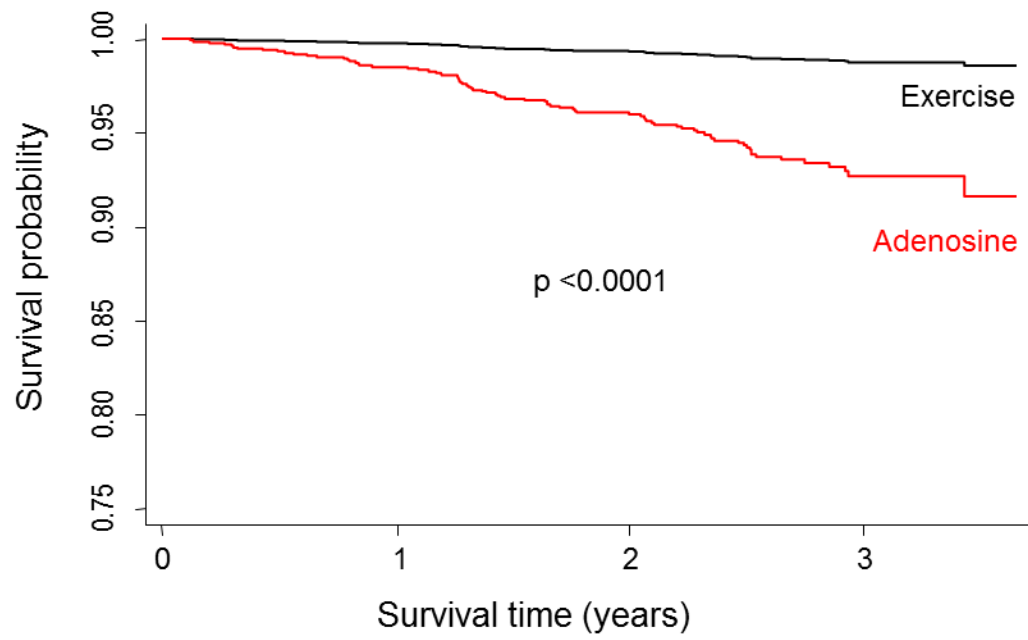


**Figure 4.** Example SPECT image and quantitative polar map. 59 years old female in whom an event occurred with normal visual scan (SSS%myo 0%) but probably normal (minimal perfusion defect) by quantification with sTPD 4%.



Adjusted for age, gender, risk factors, prior CAD and angina symptoms

**Figure 5.** Kaplan-Meier survival curves comparing risk adjusted outcomes in the exercise vs. adenosine patients.

Table 1

## Baseline variables

	Total (n = 1613)	Alive (n = 1534)	Death (n = 79)	p value
Age, years	60 ± 13	60 ± 13	69 ± 13	<0.0001
Men	919 (57%)	874 (57%)	45 (57%)	0.9
Prior CAD	295 (18%)	272 (18%)	23 (29%)	0.01
Previous MI	146 (9%)	133 (9%)	13 (16%)	0.02
Body mass index, kg/m <sup>2</sup>	29 ± 8	29 ± 8	29 ± 11	0.8
CAD risk factors				
Hypertension	1009 (63%)	945 (62%)	64 (81%)	0.001
Diabetes	347 (22%)	323 (21%)	24 (30%)	0.04
Hypercholesterolemia	945 (59%)	901 (59%)	44 (56%)	0.6
Family history	254 (16%)	247 (16%)	7 (9%)	0.09
Smoking	117 (7%)	111 (7%)	6 (8%)	0.9
Symptom class				
Asymptomatic	496 (31%)	463 (30%)	33 (42%)	0.03
Nonanginal pain	67 (4%)	61 (4%)	6 (8%)	0.1
Atypical angina	809 (50%)	786 (51%)	23 (29%)	<0.001
Typical angina	47 (3%)	45 (3%)	2 (3%)	0.8
Shortness of breath	194 (12%)	179 (12%)	15 (19%)	0.05
Type of stress				
Adenosine stress	793 (49%)	722 (47%)	71 (90%)	<0.001
Isotope type				
Rest/stress MIBI	1009 (62%)	963 (63%)	46 (58%)	0.4
Stress TL/rest MIBI	544 (34%)	512 (33%)	32 (41%)	0.2
Rest TL/stress MIBI	60 (4%)	59 (4%)	1 (1%)	0.2
sTPD, %	3.4 ± 5.7	3.3 ± 5.7	5.3 ± 5.8	0.003
SSS%myo, %	2.0 ± 5.6	1.9 ± 5.5	4.4 ± 6.6	<0.001
iTPD, %	1.8 ± 2.7	1.8 ± 2.6	3.0 ± 3.0	<0.001
SDS%myo, %	1.0 ± 2.5	0.9 ± 2.4	2.4 ± 3.6	<0.001
stress LVEF, %	62 ± 12	63 ± 12	58 ± 13	<0.001
rest LVEF, %	61 ± 14	61 ± 13	59 ± 15	0.003

CAD, coronary artery disease; MI, myocardial infarction; MIBI, <sup>99m</sup>Tc-sestamibi; TL, <sup>201</sup>Tl; sTPD, stress total perfusion deficit; SSS%myo, percentage of abnormal myocardium at stress; iTPD, ischemic total perfusion deficit; SDS%myo, percentage of ischemic myocardium; LVEF, left ventricular ejection fraction

**Table 2**

Comparing clinical characteristics of exercise vs. adenosine patients

	Exercise (n = 820)	Adenosine (n =793)	p value
Age, years	57 ± 12	64 ± 13	<0.0001
Men	507 (62%)	412 (52%)	<0.001
Prior CAD	102 (12%)	193 (24%)	<0.001
Previous MI	46 (6%)	100 (13%)	<0.001
Body mass index, kg/m <sup>2</sup>	28 ± 6	30 ± 9	<0.0001
CAD risk factors			
Hypertension	429 (52%)	580 (73%)	<0.001
Diabetes	122 (15%)	225 (28%)	<0.001
Hypercholesterolemia	481 (59%)	464 (59%)	0.9
Family history	149 (18%)	105 (13%)	0.007
Smoking	64 (8%)	53 (7%)	0.4
Symptom class			
Asymptomatic	229 (28%)	267 (34%)	0.01
Nonanginal pain	23 (3%)	44 (6%)	0.006
Atypical angina	469 (57%)	340 (43%)	<0.001
Typical angina	19 (2%)	28 (4%)	0.1
Shortness of breath	80 (10%)	114 (14%)	0.004
Isotope type			
Rest/stress MIBI	515 (63%)	494 (62%)	0.8
Stress Tl/rest MIBI	279 (34%)	265 (33%)	0.8
Rest Tl/stress MIBI	26 (3%)	34 (4%)	0.2
sTPD, %	2.1 ± 3.8	4.7 ± 7.0	<0.001
SSS%myo, %	1.0 ± 3.7	3.1 ± 6.9	<0.001
iTPD, %	1.3 ± 2.1	2.4 ± 3.1	<0.001
SDS%myo, %	0.5 ± 1.8	1.5 ± 3.1	<0.001
stress LVEF, %	64 ± 11	60 ± 13	<0.001
rest LVEF, %	62 ± 12	60 ± 14	<0.001

**Table 3**

Univariable Cox regression analysis for prediction of death

	<b>Hazard Ratio</b>	<b>95% CI</b>	<b>p value</b>
Age	1.05	1.03 – 1.07	<0.001
Male	0.99	0.64 – 1.55	0.9
Hypertension	2.55	1.45 – 4.48	0.001
Diabetes	1.61	0.99 – 2.60	0.05
Hypercholesterolemia	0.86	0.55 – 1.35	0.5
Smoking	1.03	0.45 – 2.37	0.9
Family History	0.52	0.24 – 1.13	0.1
Prior CAD	1.87	1.15 – 3.04	0.01
Adenosine stress	9.67	4.66 – 20.09	<0.001
sTPD 0%	1.00 (ref)	-	-
sTPD 1–4%	2.21	1.18 – 4.16	0.01
sTPD 5–10%	3.59	1.69 – 7.64	0.001
sTPD >10%	6.14	2.89 – 13.08	<0.001
SSS%myo 0%	1.00 (ref)	-	-
SSS%myo 1–4%	1.65	0.92 – 2.94	0.09
SSS%myo 5–10%	3.34	1.70 – 6.58	<0.001
SSS%myo >10%	4.46	2.47 – 8.06	<0.001
iTPD 0%	1.00 (ref)	-	-
iTPD 1–4%	1.56	0.94 – 2.59	0.09
iTPD 5–10%	3.67	1.95 – 6.90	<0.001
iTPD >10%	2.66	0.81 – 8.76	0.1
SDS%myo 0%	1.00 (ref)	-	-
SDS%myo 1–4%	1.95	1.05 – 3.60	0.03
SDS%myo 5–10%	4.05	2.23 – 7.35	<0.001
SDS%myo >10%	3.62	1.31 – 10.05	0.01



**Table 4**

Multivariable Cox regression analysis for prediction of death

	<b>Hazard ratio</b>	<b>95% CI</b>	<b>p value</b>
<b>Model 1</b>			
sTPD 0%	1.00 (ref)	-	-
sTPD 1–4%	1.51	0.79 – 2.89	0.2
sTPD 5–10%	1.93	0.88 – 4.24	0.1
sTPD >10%	3.03	1.30 – 7.09	0.01
<b>Model 2</b>			
SSS%myo 0%	1.00 (ref)	-	-
SSS%myo 1–4%	1.06	0.58 – 1.92	0.9
SSS%myo 5–10%	2.17	1.05 – 4.50	0.04
SSS%myo >10%	2.51	1.23 – 5.14	0.01
<b>Model 3</b>			
iTPD 0%	1.00 (ref)	-	-
iTPD 1–4%	1.16	0.69 – 1.94	0.6
iTPD 5–10%	1.89	0.97 – 3.66	0.06
iTPD >10%	1.48	0.43 – 5.11	0.5
<b>Model 4</b>			
SDS%myo 0%	1.00 (ref)	-	-
SDS%myo 1–4%	1.24	0.66 – 2.32	0.5
SDS%myo 5–10%	2.87	1.48 – 5.53	0.002
SDS%myo >10%	1.66	0.56 – 4.86	0.4

Each model was adjusted by age, gender, hypertension, diabetes, prior CAD, angina symptoms and type of stress.